# References


[1] Vasilescu, M. and Terzopoulos, D. Muiltilinear analysis of image ensembles: Tensorfaces. In Proc. of European Conference on Computer Vision (ECCV) (2002): 447–460.

[2] Vasilescu, M. and Terzopoulos, D. Multilinear subspace analysis of image ensembles. In Proc. of Computer Vision and Pattern Recognition (CVPR) 2 (2003): 93–99.

[3] Huang, T. S. and Tsan, R. Y. Multiple frame image restoration and registration. In Advances in Computer Vision and Image Processing 1 (1982): 317–339.

[4] Schultz, R. and Stevenson, R. A bayseian approach to image expansion for improved definition. IEEE Trans. Image Processing 3 , 3 (1994): 233–242.

[5] Schultz, R. and Stevenson, R. Extractionn of high-resolution frames from video sequences. IEEE Trans. Image Processing 5 , 6 (1996): 996–1011.

[6] Elad, M. and Feuer, A. Restoration of a single superresolution image from several blurred, noisy, and undersampled measured images. IEEE Trans. Image Processing 6 , 12 (1997): 1646–1658.

[7] Elad, M. and Feuer, A. Superresolution restoration of an image sequence: adaptive filtering approach. IEEE Trans. Image Processing 8 , 3 (1999): 387–395.

[8] Elad, M. and Feuer, A. Super-resolution reconstruction of image sequences. IEEE Trans. on Pattern Analysis and Machine Intelligence 21 , 9 (1999): 817–834.

[9] Patti, A., Sezan, M., and Tekalp, A. Super-resolution video reconstruction with arbitrary sampling latices and nonzero aperture time. IEEE Trans. Image Processing 6 , 8 (1997): 1064–1076.

[10] Bascle, B., Blake, A., and Zisserman, A. Motion deblurring and super-resolution from an image sequence. Proc. Fourth European Conf. Computer Vision (1996): 573–581.

[11] Patanavijit, V. and Jitapunkul, S. A lorentzian stochastic estimation for a robust iterative multiframe super-resolution reconstruction with lorentzian-tikhonov regularization. EURASIP Journal on Advances in Signal Processing 2007 (2007): 21.

[12] Kim, S., Bose, N., and Valenzuela, H. Recursive reconstruction of high resolution image from noisy undersampled multiframes. IEEE Trans. Acoustics, Speech and Signal Process 38 (1990): 1013–1027.

[13] Kim, S. and Wen-Yu, S. Recursive high-resolution reconstruction of blurred multiframe images. IEEE Trans. Image Process. 2 (1993): 534–539.

[14] Combettes, P. and Civanlar, M. The foundations of set theoretic estimation. Proc. IEEE Int. Conf. on Acoustics, Speech, and Signal Processing (ICASSP) 4 , Apr. (1991): 2921–2924.

[15] Vandewalle, P., Ssstrunk, S., and Vetterli, M. Double resolution from a set of aliased images. Proc. SPIE Electronic Imaging 2004: Sensors and Camera Systems for Scientific, Industrial, and Digital Photography Applications V (Jan. 2004): 374–382.

[16] Vandewalle, P., Sbaiz, L., Vetterli, M., and Ssstrunk, S. Super-resolution from highly undersampled images. Proc. IEEE Int. Conf. on Image Processing (ICIP) 1 (Sept. 2005): 889–892.

[17] Vandewalle, P., Ssstrunk, S., and Vetterli, M. A frequency domain approach to registration of aliased images with application to super resolution. EURASIP J. Appl. Signal Process. (2006): 14.

[18] Capel, D. P. and Zisserman, A. Super-resolution from multiple views using learnt image models. In Proc. IEEE Int. Conf. on Computational Vision Pattern Recognition (CVPR) (2001): 627–634.

[19] Baker, S. and Kanade, T. Hallucinating faces. IEEE Int. Conf. Automatic Face and Gesture Recognition.

[20] Hardie, R., Barnard, K., and Armstrong, E. Joint map registration and high-resolution image estimation using a sequence of undersampled images. IEEE Trans. Image Processing 6 (June 1977): 1621–1633.

[21] Bonet, J. D. Multiresolution sampling procedure for analysis and synthesis of texture images. Proc. SIGGRAPH 97 (August 1997): 361–368.

[22] Bonet, J. D. and Viola, P. A nonparametric multi-scale statistical model forneutr al images. Proc. Advances Neutral Inf. Process.

[23] Kim, S. and Su, W. Recursive reconstruction of high-resolution reconstruction of blurred multiframes images. IEEE Trans. Image Processing 2 (June 1993): 534–539.

[24] Penev, P. S. and Sirovich, L. The global dimensionality of face space. Proc. IEEE Int. Conf. Automatic Face and Gesture Recognition (2000): 264–270.

[25] Ma, X., Zhang, J., and Qi, C. Position-based face hallucination method. IEEE International Conference on Multimedia and Expo, 2009 (ICME). (2009): 290–293.

[26] Ma, X., Zhang, J., and Qi, C. An example-based two-step face hallucination method through coefficient learning. Image Analysis and Recognition :Lecture Notes in Computer Science. 5627 (2009): 471–480.

[27] Freeman, W. T. and Pasztor, E. C. Learning low-level vision. IEEE Int. Conf. Computer Vision (ICCV).

[28] Baker, S. and Kanade, T. Limits on super-resolution and how to break them. IEEE Transactions on Pattern Analysis and Machine Intelligence (PAMI). 24 , 9 (2002): 1167–1183.

[29] Liu, C., Zhang, C., and Shum, H. A two-step approach to hallucinating faces: Global parametric model and local nonparametric model. In Proc. IEEE Conf. Computer Vision and Pattern Recognition (CVPR) (2001): 192–198.

[30] Wang, X. and Tang, X. Hallucinating face by eigentransformation. IEEE Trans. on Systems,Man and Cybernetics 35 , 3 (2005): 425–434.

[31] Tang, X. and Wang, X. Face sketch recognition. IEEE Trans. on Circuits, Systems, and Video Technology 14 , 1 (2004): 50–57.

[32] Chang, H., Yeung, D., and Xiong, Y. Super-resolution through neighbor embedding. In Proc. of SIGGRAPH 1 (2004): 275–282.

[33] Wu, J. and Trivedi, M. M. A regression model in tensorpca subspace for face image super-resolution reconstruction. In Proc. IEEE Conf. Computer Vision and Pattern Recognition (CVPR) 3 (2006): 627–630.

[34] Chakrabarti, A., Rajagopalan, A., and Chellappa, R. Super-resolution of face images using kernel pca-based prior. IEEE Trans. on Multimedia 9 (2007): 888–892.

[35] Ogawa, T. and Haseyama, M. Kernel pca-based resolution enhancement approach of still images using different levels of pyramid structure. In Proc. IEEE Int. Conf. on Acoustics, Speech and Signal Processing (ICASSP) 9 (April 2008): 1293–1296.

[36] Jia, K. and Gong, S. Multi-modal tensor face for simultaneous superresolution and recognition. In Proc. IEEE Int. Conf. Computer Vision (ICCV) (2005): 1683–1690.

[37] Jia, K. and Gong, S. Multi-resolution tensor for facial expression hallucination. In Proc. IEEE Conf. Computer Vision and Pattern Recognition (CVPR) (2006): 395–402.

[38] Jia, K. and Gong, S. Generalized face super-resolution. IEEE Trans. Image Processing 17 , 6 (2008): 873–886.

[39] Ma, X., Huang, H., Wang, S., and Qi, C. A simple approach to multiview face hallucination. Signal Processing Letters, IEEE 17 (June 2010): 579–582.

[40] Carroll, J. and Chang, J. Analysis of individual differences in multidimensional scaling via an n-way generalization of eckart-young decomposition. Psychometrika 35 (1970): 283–319.

[41] A. Kapteyn, H. N. and T.Wansbeek An approach to n-mode components analysis. Psychometrika 51 (1986): 269–275.

[42] Kroonenbergand, P. M. and Leeuw, J. Principal component analysis of three-mode data by means of alternating least squares algorithms. Psychometrika 45 (1980): 69–97.

[43] Kruskal, J. B. Three-way arrays: Rank and uniqueness of trilinear decompositions, with application to arithmetic complexity and statistics. Linear Algebra Appl 18 (1977): 95–138.

[44] Leibovici, D. and Sabatier, R. A singular value decomposition of a k-way array for principal component analysis of multiway data, pta-k. Linear Algebra Appl (1998): 307–329.

[45] Zhangand, T. and Golub, G. H. Some mathematical notes on three-mode factor analysis. SIAM J. Matrix Anal. Appl 23 (2001): 534–550.

[46] Tucker, L. R. Some mathematical notes on three-mode factor analysis. Psychometrika 31 (1966): 279–311.

[47] Lathauwer, L., Moor, B., and Vandewalle, J. Multilinear singular value tensor decompositions. SIAM Journal on Matrix Analysis and Applications 21 (April 2008): 1253–1278.

[48] Kolda, T. G. Orthogonal tensor decompositions.. SIAM Journal on Matrix Analysis and Applications 23 (July 2001): 243–255.

[49] Shah, N. R. and Zakhor, A. Resolution enhancement of color video sequences. IEEE Trans. Image Proc. 8 (June 1999): 879–885.

[50] Tom, B. C. and Katsaggelos, A. Resolution enhancement of monochrome and color video using motion compensation. IEEE Trans. Image Proc. 10 (Feb 2001): 278–287.

[51] Irani, M. and Peleg, S. Improving resolution by image registration. CVGIP: Graph. Models Image Proc. 53 (1991): 231–239.

[52] Patil, V. H., Bormane, D. S., and Patil, H. K. Color super resolution image reconstruction. In Proc. IEEE Int. Conf. on Computational Intelligence and Multimedia Application 6 (2007): 366–370.

[53] El-Yamany, N. A. and Papamichalis, P. E. Robust color image superresolution: An adaptive m-estimation framework. EURASIP Journal on Image and Video Proc.

[54] Kimmel, R. Demosaicing: Image reconstruction from color ccd samples. IEEE Trans. Image Proc. 8 (Sep 1999): 1221–1228.

[55] Trussell, H. and Hartwig, R. E. Mathematics for demosaicking. IEEE Trans. Image Proc. 11 (April 2002): 485–492.

[56] Farsiu, S., Elad, M., and Milanfar, P. Multiframe demosaicing and super-resolution of color images. IEEE Trans. Image Proc. 15 (Jan 2006): 141–159.

[57] Shah, N. R. and Zakhor, A. Resolution enhancement of color video sequences. IEEE Trans. Image Proc. 8 (June 1999): 879–885.

[58] Tom, B. C. and Katsaggelos, A. K. Resolution enhancement of monochrome and color video using motion compensation. IEEE Trans. Image Proc. 10 (Feb. 2001): 278–287.

[59] Yang, J., Zhang, D., Frangi, A. F., , and Yang, J. Two-dimensional pca: A new approach to appearance-based face representation and recognition. IEEE Trans. Pattern Anal. Mach. Intell 26 (Jan. 2004): 131-137.

[60] Vasilescu, M. A. O. and Terzopoulos, D. Multilinear subspace analysis for image ensembless. In Proc. of Computer Vision and Pattern Recognition (CVPR) 2 (June 2003): 93–99.

[61] Vasilescu, M. A. O. and Terzopoulos, D. Multilinear analysis of image ensembles: Tensorfaces. In Proc. 7th Eur. Conf. Comput. Vis (ECCV) (May 2002): 447–460.

[62] Ye, J., Janardan, R., and Li, Q. Gpca: An efficient dimension reduction scheme for image compression and retrieval. In Proc. 10th ACM SIGKDD Int. Conf. Knowl. Discovery Data Mining (2004): 354-363.

[63] Lu, H., Plataniotis, K. N. K., and Venetsanopoulos, A. N. MPCA: Multilinear principal component analysis of tensor objects. IEEE Transactions on Neural Networks 19 , 1 (2008): 18–39.

[64] Yang, J., Zhang, D., and Frangi, A. F. Two-dimensional pca: A new approach to appearance-based face representation and recognition. IEEE Trans. Pattern Anal. Mach. Intell 26 (Jan. 2004): 131-137.

[65] Cohen, J. and Kappauf, W. Metameric color stimuli, fundamental metamers, and wyszeckis metameric blacks. Amer. J. Psychol 95 , 4 (1982): 537-564.

[66] Horn, B. Exact reproduction of colored images. Computer Vision, Graph. Image Processing 26 (1984): 135-167.

[67] Wandell, B. The synthesis and analysis of color images. IEEE Trans. Pattern Anal. Machine Intell 9 (Jan. 1987): 2-13.

[68] Trussell, H. Applications of set theoretic methods to color systems. Color Res. Applicat 16 (Feb. 1991): 31-41.

[69] Trussell, H. Dsp solutions run the gamut for color systems. IEEE Signal Processing Mag 10 (Apr. 1993): 8-23.

[70] Sharma, G. and Trussell, H. Digital color processing. IEEE Trans. Image Processing 6 , 7 (1997): 901-932.

[71] Plataniotis, K. N. and Venetsanopoulos, A. N. Color image processing and applications. Berlin, Germany: Springer-Verlag.

[72] Koschan, A. and Abidi, M. Detection and classification of edges in color images. IEEE Signal Processing Mag 22 (Jan. 2005): 64-73.

[73] Lukac, R., Smolka, B., Martin, K., Plataniotisand, K., and Venetsanopoulos, A. Vector filtering for color imaging. IEEE Signal Processing Mag 22 (Jan. 2005): 74-86,.

[74] Baqai, F., Lee, J., Agar, A., and Allebach, J. Digital color halftoning. IEEE Signal Processing Mag 22 (Jan. 2005): 87-96.

[75] Vrhel, M. and Trussell, H. Color printer characterization in MATLAB. International Conference on Image Processing (ICIP) 1 (Sept. 2002): 457-460.

[76] Kay and M., S. Fundamentals of statistical signal processing: Estimation theory.. Prentice Hall (1993): .

[77] Hardie, R. C., Barnard, K. J., and Armstrong, E. E. Joint map registration and high-resolution image estimation using a sequence of undersampled images. IEEE Trans. Image Processing 6 (Dec. 1997): 1621-1633.

[78] Phillips, P. J., Wechsler, H., Huang, J., and Rauss, P. The FERET database and evaluation procedure for face recognition algorithms. Image and Vision Computing 16 , 5.

[79] Phillips, P. J., Moon, H., Rizvi, S. A., and Rauss, P. J. The FERET evaluation methodology for face recognition algorithms. IEEE Transactions on Pattern Analysis and Machine Intelligence (PAMI). 22.

[80] Liu, C., Shum, H. Y., and Zhang, C. S. A two-step approach to hallucinating faces: Global parametric model and local nonparametric model. In Proc. of IEEE computer society conference on computer vision and pattern recognition (2001): 192–198.

# Appendices

# Appendix A
# List of Abbreviations



| | |
|---|---|
| 2DPCA | Two-Dimensional Principal Component Analysis |
| HOSVD | High Order Singular Value Decomposition |
| LR | Low Resolution |
| HR | High Resolution |
| ICCA | Image Cross-Covariance Analysis |
| LDA | Linear Discriminant Analysis |
| MPCA | Multilinear Principal Component Analysis |
| NN | The nearest neighbor classifier |
| PCA | Principal Component Analysis |
| RSM | Random Subspace Method |
| SAR | Synthetic Aperture Radar |
| SSS | Small Sample Size Problem |
| SVD | Singular Value Decomposition |
| HSV | Hue, Saturation, Value |
| LLE | Locally Linear Embedding |
| MRF | Markov Random Field |
| MFH | multiview face hallucination |

# Appendix B
# Some Experimental Results

Table 1 PSNR results of Fig. 2 with a linear regression model in MPCA method

| Case | 90 percent | 95 percent | 100 percent |
|---|---|---|---|
| 1) $the\ 1^{st}\ row$ | 31.49 dB | 31.52 dB | 32.57 dB |
| 2) $the\ 2^{nd}\ row$ | 31.40 dB | 31.43 dB | 31.61 dB |
| 3) $the\ 3^{rd}\ row$ | 24.61 dB | 24.67 dB | 26.89 dB |
| 4) $the\ 4^{th}\ row$ | 27.45 dB | 27.52 dB | 27.87 dB |
| 5) $the\ 5^{th}\ row$ | 35.60 dB | 35.61 dB | 35.71 dB |
| 6) $the\ 6^{th}\ row$ | 26.31 dB | 26.39 dB | 26.77 dB |
| 7) $the\ 7^{th}\ row$ | 27.24 dB | 27.40 dB | 29.61 dB |
| 8) $the\ 8^{th}\ row$ | 34.34 dB | 34.55 dB | 34.68 dB |
| 9) $the\ 9^{th}\ row$ | 36.53 dB | 36.67 dB | 37.33 dB |
| 10) $the\ 10^{th}\ row$ | 42.74 dB | 42.79 dB | 43.56 dB |
| 11) $the\ 11^{th}\ row$ | 28.28 dB | 28.30 dB | 28.63 dB |
| 12) $the\ 12^{th}\ row$ | 33.69 dB | 33.71 dB | 33.96 dB |
| 13) $the\ 13^{th}\ row$ | 26.56 dB | 26.73 dB | 26.85 dB |
| 14) $the\ 14^{th}\ row$ | 31.90 dB | 31.96 dB | 32.25 dB |

Table 2 PSNR results of Fig. 3 with a linear regression model in MPCA method

| Case | 90 percent | 95 percent | 100 percent |
|---|---|---|---|
| 1) *the* $1^{st}$ *row* | 31.52 dB | 31.58 dB | 32.62 dB |
| 2) *the* $2^{nd}$ *row* | 31.43 dB | 31.45 dB | 31.69 dB |
| 3) *the* $3^{rd}$ *row* | 24.67 dB | 24.73 dB | 26.96 dB |
| 4) *the* $4^{th}$ *row* | 27.49 dB | 27.55 dB | 27.95 dB |
| 5) *the* $5^{th}$ *row* | 35.61 dB | 35.63 dB | 35.75 dB |
| 6) *the* $6^{th}$ *row* | 26.36 dB | 26.44 dB | 26.90 dB |
| 7) *the* $7^{th}$ *row* | 27.25 dB | 27.47 dB | 29.70 dB |
| 8) *the* $8^{th}$ *row* | 34.39 dB | 34.58 dB | 34.86 dB |
| 9) *the* $9^{th}$ *row* | 36.62 dB | 36.70 dB | 37.45 dB |
| 10) *the* $10^{th}$ *row* | 42.75 dB | 42.83 dB | 43.58 dB |
| 11) *the* $11^{th}$ *row* | 28.35 dB | 28.39 dB | 28.77 dB |
| 12) *the* $12^{th}$ *row* | 33.70 dB | 33.74 dB | 34.06 dB |
| 13) *the* $13^{th}$ *row* | 26.59 dB | 26.75 dB | 26.95 dB |
| 14) *the* $14^{th}$ *row* | 31.99 dB | 32.03 dB | 32.35 dB |

Table 3 PSNR results of Fig. 4 with a linear regression model in MPCA method

| Case | 90 percent | 95 percent | 100 percent |
|---|---|---|---|
| 1) *the* $1^{st}$ *row* | 30.22 dB | 30.35 dB | 30.87 dB |
| 2) *the* $2^{nd}$ *row* | 30.13 dB | 30.24 dB | 30.54 dB |
| 3) *the* $3^{rd}$ *row* | 23.56 dB | 23.61 dB | 23.97 dB |
| 4) *the* $4^{th}$ *row* | 26.24 dB | 26.39 dB | 26.98 dB |
| 5) *the* $5^{th}$ *row* | 35.12 dB | 35.24 dB | 35.54 dB |
| 6) *the* $6^{th}$ *row* | 25.86 dB | 25.97 dB | 26.25 dB |
| 7) *the* $7^{th}$ *row* | 26.89 dB | 27.06 dB | 27.66 dB |
| 8) *the* $8^{th}$ *row* | 31.03 dB | 31.51 dB | 32.18 dB |
| 9) *the* $9^{th}$ *row* | 33.37 dB | 33.92 dB | 34.85 dB |
| 10) *the* $10^{th}$ *row* | 41.12 dB | 41.56 dB | 41.94 dB |
| 11) *the* $11^{th}$ *row* | 27.52 dB | 27.78 dB | 28.01 dB |
| 12) *the* $12^{th}$ *row* | 31.76 dB | 32.12 dB | 32.72 dB |
| 13) *the* $13^{th}$ *row* | 26.08 dB | 26.23 dB | 26.54 dB |
| 14) *the* $14^{th}$ *row* | 30.67 dB | 30.86 dB | 31.15 dB |

Table 4 PSNR results of Fig. 5 with a linear regression model in MPCA method

| Case | 90 percent | 95 percent | 100 percent |
|---|---|---|---|
| 1) $the\ 1^{st}\ row$ | 31.58 dB | 31.61 dB | 32.75 dB |
| 2) $the\ 2^{nd}\ row$ | 31.57 dB | 31.63 dB | 31.88 dB |
| 3) $the\ 3^{rd}\ row$ | 24.70 dB | 24.78 dB | 26.87 dB |
| 4) $the\ 4^{th}\ row$ | 27.53 dB | 27.58 dB | 27.92 dB |
| 5) $the\ 5^{th}\ row$ | 35.64 dB | 35.73 dB | 35.94 dB |
| 6) $the\ 6^{th}\ row$ | 26.43 dB | 26.52 dB | 26.98 dB |
| 7) $the\ 7^{th}\ row$ | 27.47 dB | 27.71 dB | 28.13 dB |
| 8) $the\ 8^{th}\ row$ | 34.48 dB | 34.67 dB | 34.96 dB |
| 9) $the\ 9^{th}\ row$ | 36.68 dB | 36.75 dB | 37.49 dB |
| 10) $the\ 10^{th}\ row$ | 42.79 dB | 42.87 dB | 43.64 dB |
| 11) $the\ 11^{th}\ row$ | 28.37 dB | 28.41 dB | 28.83 dB |
| 12) $the\ 12^{th}\ row$ | 33.75 dB | 33.78 dB | 34.19 dB |
| 13) $the\ 13^{th}\ row$ | 26.65 dB | 26.88 dB | 27.24 dB |
| 14) $the\ 14^{th}\ row$ | 31.98 dB | 32.11 dB | 32.52 dB |

Table 5 PSNR results of Fig. 6 with a linear regression model in tensorPCA method

| Case | 90 percent | 95 percent | 100 percent |
|---|---|---|---|
| 1) $the\ 1^{st}\ row$ | 31.19 dB | 31.22 dB | 32.27 dB |
| 2) $the\ 2^{nd}\ row$ | 31.06 dB | 31.09 dB | 31.21 dB |
| 3) $the\ 3^{rd}\ row$ | 24.31 dB | 24.33 dB | 26.52 dB |
| 4) $the\ 4^{th}\ row$ | 27.20 dB | 27.32 dB | 27.47 dB |
| 5) $the\ 5^{th}\ row$ | 35.34 dB | 35.41 dB | 35.62 dB |
| 6) $the\ 6^{th}\ row$ | 26.02 dB | 26.03 dB | 26.39 dB |
| 7) $the\ 7^{th}\ row$ | 27.11 dB | 27.32 dB | 29.48 dB |
| 8) $the\ 8^{th}\ row$ | 34.26 dB | 34.32 dB | 34.38 dB |
| 9) $the\ 9^{th}\ row$ | 36.03 dB | 36.09 dB | 36.56 dB |
| 10) $the\ 10^{th}\ row$ | 42.63 dB | 42.71 dB | 43.13 dB |
| 11) $the\ 11^{th}\ row$ | 28.14 dB | 28.23 dB | 28.51 dB |
| 12) $the\ 12^{th}\ row$ | 33.07 dB | 33.29 dB | 33.78 dB |
| 13) $the\ 13^{th}\ row$ | 26.29 dB | 26.45 dB | 26.68 dB |
| 14) $the\ 14^{th}\ row$ | 31.53 dB | 31.72 dB | 32.18 dB |

Table 6 PSNR results of Fig. 7 with a linear regression model in tensorPCA method

| Case | 90 percent | 95 percent | 100 percent |
|---|---|---|---|
| 1) $the\ 1^{st}\ row$ | 31.36 dB | 31.44 dB | 32.53 dB |
| 2) $the\ 2^{nd}\ row$ | 31.14 dB | 31.32 dB | 31.44 dB |
| 3) $the\ 3^{rd}\ row$ | 24.49 dB | 24.52 dB | 26.78 dB |
| 4) $the\ 4^{th}\ row$ | 27.36 dB | 27.42 dB | 27.68 dB |
| 5) $the\ 5^{th}\ row$ | 35.50 dB | 35.61 dB | 35.71 dB |
| 6) $the\ 6^{th}\ row$ | 26.19 dB | 26.25 dB | 26.63 dB |
| 7) $the\ 7^{th}\ row$ | 26.89 dB | 27.11 dB | 28.95 dB |
| 8) $the\ 8^{th}\ row$ | 34.03 dB | 34.31 dB | 34.56 dB |
| 9) $the\ 9^{th}\ row$ | 36.43 dB | 36.52 dB | 37.01 dB |
| 10) $the\ 10^{th}\ row$ | 42.21 dB | 42.42 dB | 43.19 dB |
| 11) $the\ 11^{th}\ row$ | 28.09 dB | 28.27 dB | 28.63 dB |
| 12) $the\ 12^{th}\ row$ | 33.25 dB | 33.47 dB | 33.87 dB |
| 13) $the\ 13^{th}\ row$ | 26.18 dB | 26.42 dB | 26.74 dB |
| 14) $the\ 14^{th}\ row$ | 31.27 dB | 31.78 dB | 32.04 dB |

Table 7 PSNR results of Fig. 8 with a linear regression model in tensorPCA method

| Case | 90 percent | 95 percent | 100 percent |
|---|---|---|---|
| 1) $the\ 1^{st}\ row$ | 30.14 dB | 30.25 dB | 30.56 dB |
| 2) $the\ 2^{nd}\ row$ | 30.01 dB | 30.11 dB | 30.26 dB |
| 3) $the\ 3^{rd}\ row$ | 23.31 dB | 23.44 dB | 23.62 dB |
| 4) $the\ 4^{th}\ row$ | 26.01 dB | 26.22 dB | 26.45 dB |
| 5) $the\ 5^{th}\ row$ | 34.51 dB | 34.77 dB | 34.92 dB |
| 6) $the\ 6^{th}\ row$ | 25.64 dB | 25.71 dB | 25.97 dB |
| 7) $the\ 7^{th}\ row$ | 26.21 dB | 26.83 dB | 27.19 dB |
| 8) $the\ 8^{th}\ row$ | 30.92 dB | 31.20 dB | 31.85 dB |
| 9) $the\ 9^{th}\ row$ | 33.18 dB | 33.54 dB | 34.17 dB |
| 10) $the\ 10^{th}\ row$ | 40.68 dB | 40.94 dB | 41.37 dB |
| 11) $the\ 11^{th}\ row$ | 27.36 dB | 27.52 dB | 27.78 dB |
| 12) $the\ 12^{th}\ row$ | 31.61 dB | 31.99 dB | 32.32 dB |
| 13) $the\ 13^{th}\ row$ | 25.89 dB | 25.97 dB | 26.02 dB |
| 14) $the\ 14^{th}\ row$ | 30.11 dB | 30.24 dB | 30.79 dB |

Table 8 PSNR results of Fig. 9 with a linear regression model in tensorPCA method

| Case | 90 percent | 95 percent | 100 percent |
|---|---|---|---|
| 1) $the\ 1^{st}\ row$ | 31.47 dB | 31.53 dB | 32.38 dB |
| 2) $the\ 2^{nd}\ row$ | 31.32 dB | 31.49 dB | 31.74 dB |
| 3) $the\ 3^{rd}\ row$ | 24.56 dB | 24.62 dB | 26.31 dB |
| 4) $the\ 4^{th}\ row$ | 27.48 dB | 27.52 dB | 27.88 dB |
| 5) $the\ 5^{th}\ row$ | 35.47 dB | 35.55 dB | 35.86 dB |
| 6) $the\ 6^{th}\ row$ | 26.38 dB | 26.49 dB | 26.78 dB |
| 7) $the\ 7^{th}\ row$ | 27.41 dB | 27.63 dB | 27.99 dB |
| 8) $the\ 8^{th}\ row$ | 34.16 dB | 34.56 dB | 34.85 dB |
| 9) $the\ 9^{th}\ row$ | 36.29 dB | 36.44 dB | 37.08 dB |
| 10) $the\ 10^{th}\ row$ | 42.61 dB | 42.75 dB | 43.59 dB |
| 11) $the\ 11^{th}\ row$ | 28.08 dB | 28.26 dB | 28.73 dB |
| 12) $the\ 12^{th}\ row$ | 33.38 dB | 33.57 dB | 33.93 dB |
| 13) $the\ 13^{th}\ row$ | 26.58 dB | 26.62 dB | 27.01 dB |
| 14) $the\ 14^{th}\ row$ | 31.69 dB | 32.05 dB | 32.46 dB |

Figure 1 Some original high-resolution color face images ($30 \times 30$) for testing.


Figure 2: Some of experimental results (RGB color model) with a linear regression model in MPCA method. (a) original HR images ($30 \times 30$); (b) input LR images ($15 \times 15$) with noise, motion and blur in LR images; (c) face hallucination result with 90 percent MPCA; (d) different image of face hallucination result with 90 percent MPCA; (e) face hallucination result with 95 percent MPCA; (f) different image of face hallucination result with 95 percent MPCA; (g) face hallucination result with 100 percent MPCA; (h) different image of face hallucination result with 100 percent MPCA;

(a) (b) (c) (d) (e) (f) (g) (h)

Figure 3: Some of experimental results (YCbCr color model) with a linear regression model in MPCA method. (a) original HR images ($30 \times 30$); (b) input LR images ($15 \times 15$) with noise, motion and blur in LR images; (c) face hallucination result with 90 percent MPCA; (d) different image of face hallucination result with 90 percent MPCA; (e) face hallucination result with 95 percent MPCA; (f) different image of face hallucination result with 95 percent MPCA; (g) face hallucination result with 100 percent MPCA; (h) different image of face hallucination result with 100 percent MPCA;

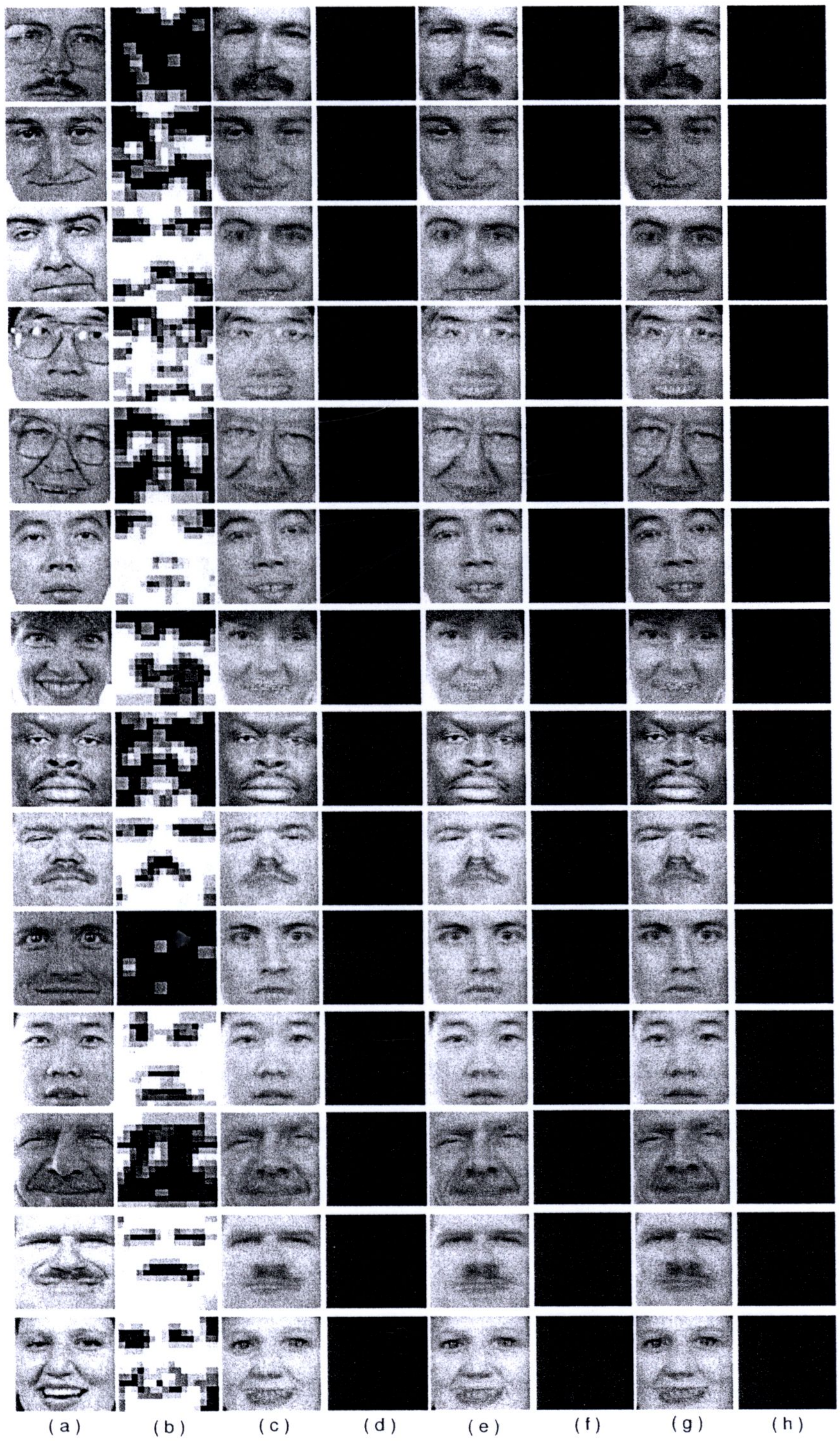


Figure 4: Some of experimental results (HSV color model) with a linear regression model in MPCA method. (a) original HR images ($30 \times 30$); (b) input LR images ($15 \times 15$) with noise, motion and blur in LR images; (c) face hallucination result with 90 percent MPCA; (d) different image of face hallucination result with 90 percent MPCA; (e) face hallucination result with 95 percent MPCA; (f) different image of face hallucination result with 95 percent MPCA; (g) face hallucination result with 100 percent MPCA; (h) different image of face hallucination result with 100 percent MPCA;


Figure 5: Some of experimental results (CIELAB color model) with a linear regression model in MPCA method. (a) original HR images $(30 \times 30)$; (b) input LR images $(15 \times 15)$ with noise, motion and blur in LR images; (c) face hallucination result with 90 percent MPCA; (d) different image of face hallucination result with 90 percent MPCA; (e) face hallucination result with 95 percent MPCA; (f) different image of face hallucination result with 95 percent MPCA; (g) face hallucination result with 100 percent MPCA; (h) different image of face hallucination result with 100 percent MPCA;


Figure 6: Some of experimental results (RGB color model) with a linear regression model in tensorPCA method. (a) original HR images ($30 \times 30$); (b) input LR images ($15 \times 15$) with noise, motion and blur in LR images; (c) face hallucination result with 90 percent tensorPCA; (d) different image of face hallucination result with 90 percent tensorPCA; (e) face hallucination result with 95 percent tensorPCA; (f) different image of face hallucination result with 95 percent tensorPCA; (g) face hallucination result with 100 percent tensorPCA; (h) different image of face hallucination result with 100 percent tensorPCA;


Figure 7: Some of experimental results (YCbCr color model) with a linear regression model in tensorPCA method. (a) original HR images ($30 \times 30$); (b) input LR images ($15 \times 15$) with noise, motion and blur in LR images; (c) face hallucination result with 90 percent tensorPCA; (d) different image of face hallucination result with 90 percent tensorPCA; (e) face hallucination result with 95 percent tensorPCA; (f) different image of face hallucination result with 95 percent tensorPCA; (g) face hallucination result with 100 percent tensorPCA; (h) different image of face hallucination result with 100 percent tensorPCA;


Figure 8: Some of experimental results (HSV color model) with a linear regression model in tensorPCA method. (a) original HR images ($30 \times 30$); (b) input LR images ($15 \times 15$) with noise, motion and blur in LR images; (c) face hallucination result with 90 percent tensorPCA; (d) different image of face hallucination result with 90 percent tensorPCA; (e) face hallucination result with 95 percent tensorPCA; (f) different image of face hallucination result with 95 percent tensorPCA; (g) face hallucination result with 100 percent tensorPCA; (h) different image of face hallucination result with 100 percent tensorPCA;


Figure 9: Some of experimental results (CIELAB color model) with a linear regression model in tensorPCA method. (a) original HR images $(30 \times 30)$; (b) input LR images $(15 \times 15)$ with noise, motion and blur in LR images; (c) face hallucination result with 90 percent tensorPCA; (d) different image of face hallucination result with 90 percent tensorPCA; (e) face hallucination result with 95 percent tensorPCA; (f) different image of face hallucination result with 95 percent tensorPCA; (g) face hallucination result with 100 percent tensorPCA; (h) different image of face hallucination result with 100 percent tensorPCA;

# Appendix C
# Publications and Presentations

Krissada Asavaskulkeit and Somchai Jitapunkul,

"Generalized color face hallucination with linear regression model in MPCA," In preparation to summit to IEICE Transaction on Information and Systems.

Krissada Asavaskulkeit and Somchai Jitapunkul,

"A Color Face Hallucination with a Linear Regression Model in MPCA," Proceeding on the 2009 International Conference on Computer Engineering and Applications (ICCEA 2009), pp. 100–104, Manila, Philippine, 6-8 June 2009.

Krissada Asavaskulkeit and Somchai Jitapunkul,

"Performance Evaluation of Color Face Hallucination with a Linear Regression Model in MPCA," Proceeding on the 2009 International Conference on Image Processing, Computer Vision, Pattern Recognition (IPCV 2009), pp. 387–392, Las Vegas Nevada, USA, 13-16 July 2009.

Krissada Asavaskulkeit and Somchai Jitapunkul,

"The Color Face Hallucination with the Linear Regression Model and MPCA in HSV Space," Proceeding on the 16th International Conference on Systems, Signals and Image Processing (IWSSIP 2009), Chalkida, Greece, 18-20 June 2009.

# Vitae

Krissada Asavaskulkeit was born in Bangkok, Thailand in 1981. He received the B.Eng. and M.Eng. degrees from the Department of Electrical Engineering at the Chulalongkorn University, Bangkok, Thailand, in 2001 and 2004 respectively. He is currently pursuing the Doctoral degree in electrical engineering at Chulalongkorn University, Bangkok, Thailand, since 2005. His research areas are digital signal processing in image processing including face hallucination and super-resolution reconstruction.